Low frequency vibrational modes related to texture in silica aerogels

J. Pelous, J.L. Sauvajol, T. Woignier, R. Vacher

Classification
Physics Abstracts
63.50 — 78.30L

Low frequency vibrational modes related to texture in silica aerogels

J. Pelous ([1]), J. L. Sauvajol ([2]), T. Woignier ([1]) and R. Vacher ([1])

([1]) Laboratoire de Science des Matériaux Vitreux (*), F-34060 Montpellier Cedex 01, France
([2]) Groupe de Dynamique des Phases Condensées (**), F-34060 Montpellier Cedex 01, France

(*Reçu le 25 septembre 1989, accepté sous forme définitive le 15 novembre 1989*)

Résumé. — Les modes de vibration basse fréquence d'aérogels de silice ont été étudiés par spectrométrie Raman. La position et la largeur des pics observés dans l'intervalle de fréquence 5 à 30 cm^{-1} apparaissent corrélées aux conditions initiales de préparation et aux traitements thermiques de densification. La fréquence du pic est proportionnelle à l'inverse du rayon de gyration des particules, déduit des mesures de diffusion élastique des neutrons aux petits angles. Ceci permet une détermination de la vitesse du son à l'intérieur des particules. De plus, la dépendance en température des spectres démontre le caractère harmonique des modes responsables du pic.

Abstract. — Low frequency vibrational modes of silica aerogels have been investigated by Raman spectrometry. The position and lineshape of the peaks observed in the range from 5 to 30 cm^{-1} appear correlated to the initial preparation conditions and to the heat treatment responsible for the densification. The maximum frequency of the peak is proportional to the inverse of the constitutive particle gyration radius deduced from small angle neutron scattering. This gives a determination of the sound velocity inside these particles. Moreover, the temperature dependence of the spectrum for one sample demonstrates the harmonic character of the modes responsible for the peak.

1. Introduction.

The vibrational dynamics of glassy networks is a matter of current research activity [1]. In particular, low-frequency modes are attracting much interest as they are related to *collective* motions of the disordered atoms. Those modes show up in acoustic properties as well as in low frequency Raman scattering of solids. They are also responsible for their low temperature thermal properties. It is well known that all of the above physical properties exhibit intriguing anomalies in glasses and, more generally, in disordered solids [2]. Highly anharmonic excitations of still unknown microscopic nature, in excess to « normal » acoustic phonons, have been proposed to describe those anomalies [3]. At low temperature, coupling of phonons with tunneling processes of those « two-level systems » (TLS) explains the non-

(*) Unité associée au CNRS 1119.
(**) Unité associée au CNRS 233.

Debye behavior of specific heat and thermal conductivity, as well as sound attenuation and dispersion [2]. At higher temperatures, the peaks of acoustic and dielectric absorption are likely to originate from thermally-activated relaxation [4]. More recently a new kind of anharmonic excitations has been proposed as an alternative explanation in disordered solids [5].

Vitreous silica is from far the most extensively studied material, as it is a common constituent of a large number of glasses. On a more fundamental viewpoint, the properties of silica glass can easily by compared to those of its stable crystalline counterparts. A microscopic model involving coupled rotations of a few SiO_4 tetrahedra has been proposed to describe the density of states deduced from inelastic neutron scattering experiments [6]. More recently, harmonic — for frequencies higher than $\simeq 0.6$ THz — and anharmonic vibrational modes — at lower frequencies — were observed in excess to propagating acoustic phonons [7]. The same model was used to give an unified description of acoustic and dielectric properties at low temperatures, as well as of neutron and Raman scattering in the low-frequency domain [8]. This picture is very attractive, but does not account for the observation of very similar anomalies in disordered materials, irrespective of their microscopic structure.

Alternatively, the concept of fractons [9] provides a possible explanation of those properties, as illustrated by Alexander *et al.* in their study of the thermal properties of quartz amorphized by neutron irradiation [10]. This was the starting point of some controversy [11] and stimulated a number of experiments [12]. In particular, Raman scattering measurements on silica gels [13], Na-colloids [14], and superionic glasses [15] have given evidence of a power-law dependence of the spectral intensity, $I(\omega) \propto \omega^{\nu}$. A calculation of the light scattering intensity in fractal media was proposed [13] from which a relation between the exponent ν, the fractal dimension D, the fracton dimension $\bar{\bar{d}}$, and the localization exponent d_{φ} [16] was derived. The results in silica gels were little sensitive to preparation conditions, and a similar behavior was also observed in Vycor, a weakly porous glass obtained in a completely different way.

The study of disordered materials having a well-established fractal structure can help to clarify the matter, inasmuch as one clearly separates (i) the test of fracton predictions for the physical properties and (ii) their adequation to glasses. Small-angle neutron [17, 18] (SANS) and X-ray [19] (SAXS) scattering experiments have demonstrated that silica aerogels are excellent examples of porous solids having a fractal structure at length scales L larger than a particle size a and smaller than a correlation length ξ. Below a and above ξ, the materials is homogeneous [18]. Previous investigations of the vibrational dynamics of these materials have given evidence of a crossover from long wavelength acoustic phonons to fractons in the Brillouin scattering frequency range, from $\simeq 0.5$ to $\simeq 5$ GHz [20]. Scattering from fractons was observed in the very low frequency Raman scattering region, typically below 300 GHz (10 cm^{-1}) [21]. These studies are relevant to the point (i) above. At larger frequencies, which can be analyzed by conventional Raman spectrometers, scattering of light originates from surface and internal modes of the *homogeneous* particles. They can give information on the structure of the peculiar glass obtained by the sol-gel route. That they are related to a possible fractality of glasses — point (ii) above — is still an open question.

In the present paper, we present the results of a low frequency Raman investigation of silica aerogels. The frequency range explored is expected up to the fracton regime [21]. We first compare the spectra obtained on two series of samples corresponding to different preparation conditions. The changes of the low frequency Raman spectrum during the process of densification to glass are also investigated. The evolution of the low frequency part of the spectrum is correlated with the variations of a, observed in SANS experiments on similar samples. The temperature dependence of the Raman intensity is also studied on one sample.

Our results demonstrate that, in the frequency range above 12 cm^{-1} ($\simeq$ 400 GHz), the excitations responsible for Raman scattering show an harmonic character.

2. Sample preparation and experimental procedure.

The aerogels were prepared by hydrolysis and polycondensation of tetramethoxysilane (TMOS), followed by hypercritical drying. Four moles of water per mole of TMOS were used. Two kinds of materials were investigated namely neutrally reacted and base catalysed samples ; in the latter case the water was brought to a normality of 0.05 of ammonia. The samples were oxidized at 500 °C in air during 15 hours. This treatment removes some residual methyl groups and decreases fluorescence lines which sometimes overlap the Raman spectra of the aerogels.

Densification was obtained by heat treatment. Four pieces of oxidized aerogel of each series were treated at 1 050 °C for various durations. The final densities of these samples are given as labels of the Raman spectra in the figures.

To observe Raman scattering from silica aerogels, a conventional experimental configuration was used. Raman experiments were performed using a « Coderg T800 » triple monochromator spectrometer. Scattering was obtained with the 5 145 nm line of an argon-ion laser (Spectra Physics type 2020), with the output power of the incident beam kept at 500 mW. The scattered light was collected in right-angle configuration and in VH polarization. The instrumental linewidth was 1 cm^{-1}. At room temperature the low frequency scattering was studied under vacuum to avoid scattering originating from air in the sample pores.

Low temperature measurements were performed in a ^4He cryostat. As silica aerogels are very poor heat conductors, the precise determination of the sample temperature becomes more and more difficult as the temperature is lowered. To improve heat exchange, the sample holder was directly immersed in liquid helium.

3. Results and discussion.

The Raman spectra $I(\omega)$ have been analyzed at room temperature for the two series of samples. Figure 1 compares the results obtained for two untreated samples, one neutrally reacted and the other prepared under basic catalysis. Here we have plotted the Raman susceptibilities, $\chi(\omega) = I(\omega)/(n(\omega) + 1)$, where $n(\omega) + 1$ is the appropriate Bose Einstein factor for Stokes scattering. The density ρ of each sample is indicated in the figure. In agreement with previous results obtained by Boukenter *et al.* on similar samples, a broad low frequency scattering is observed from the instrumental limit $\nu \simeq 7\ cm^{-1}$ up to $\simeq 100\ cm^{-1}$. The mean feature of these spectra is a well-resolved peak. Such peaks have been tentatively assigned to the lowest energy torsional mode of silica particles. The mean particle size R is related to the peak frequency by

$$\nu_{max} \simeq 0.8(v_t/2R) \tag{1}$$

where v_t is the transverse sound velocity inside the particle.

For neutrally reacted samples, the peak is broader than for the base-catalyzed ones. This effect can be related either to a polydispersity in the particle size, or to poorly defined particle surfaces. This agrees with SANS results in which a smooth crossover from bulk fractal to Porod surface scattering is observed in neutral aerogels [18].

Curves of figures 2 and 3 correspond to various stages of densification for the neutral and base catalyzed series, respectively. The behavior with increasing density is qualitatively similar for the two kinds of gels. As expected from equation (1), the peak shifts towards lower frequencies, indicating an increase of the size of the particles, and progressively disappears

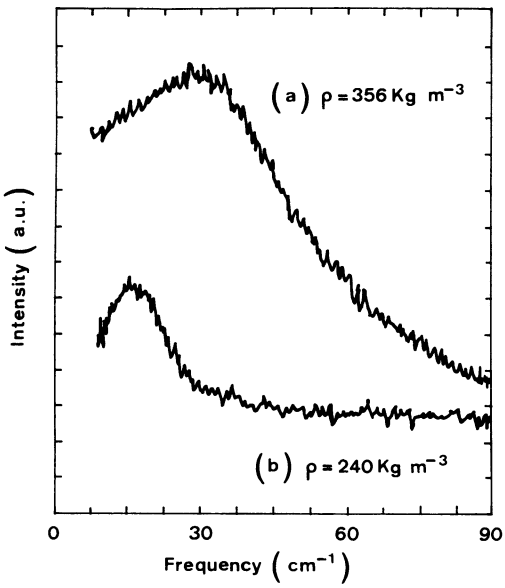

Fig. 1.

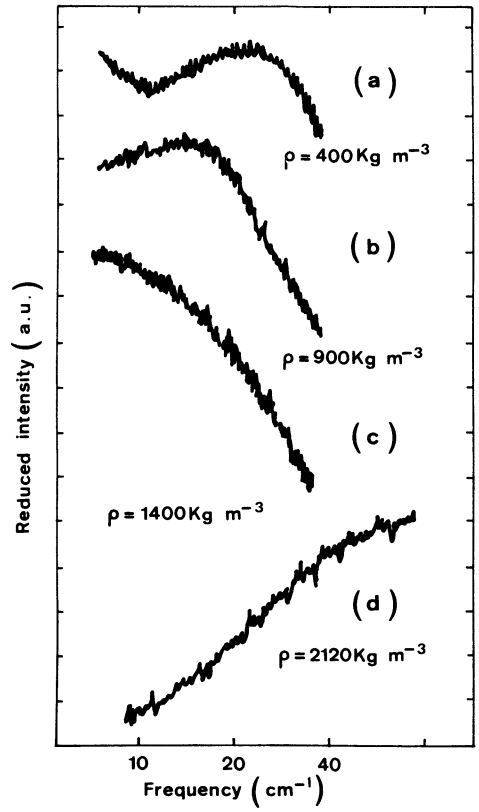

Fig. 2.

Fig. 1. — Low frequency Raman susceptibilities $\chi(\omega) = \dfrac{I(\omega)}{n(\omega)+1}$ for two untreated silica aerogels : a) neutrally reacted sample, b) base catalyzed sample.

Fig. 2. — Evolution of the low frequency Raman spectra for different times of heat treatment in neutrally reacted aerogels. The labels indicate the corresponding densities.

into the elastic line. An overintensity is still present in curve *e* of figure 3, corresponding to $\rho = 1\,600\ \text{kg.m}^{-3}$. However the maximum is now below the experimental resolution, and only allows an estimation of the higher limit of the peak position. In contrast, after the final stage of transformation of the gel into glass, the low-frequency intensity becomes very weak, as demonstrated in curve d (Fig. 2). The spectrum of the fully-densified sample is similar to that of vitreous silica.

As illustrated by the plot of ν_{max} *vs.* ρ in figure 4, the peak occurs at higher frequencies in the spectrum taken on the sample prepared under neutral conditions, than on the gel of the same density obtained under basic catalysis. This is in excellent agreement with SANS results and confirms the known result that the addition of a basic catalyst favors the formation of larger particles in the gel [22]. We observe here that these differences between catalysis conditions remain for partially densified samples ; however the gap decreases during the densification process.

It can be also noted that a linear extrapolation of the $\nu_{max}(\rho)$ curves intercept the X axis ($\nu_{max} = 0$) at the density $\rho \simeq 2\,200\ \text{kg.m}^{-3}$. This corresponds exactly to the density of

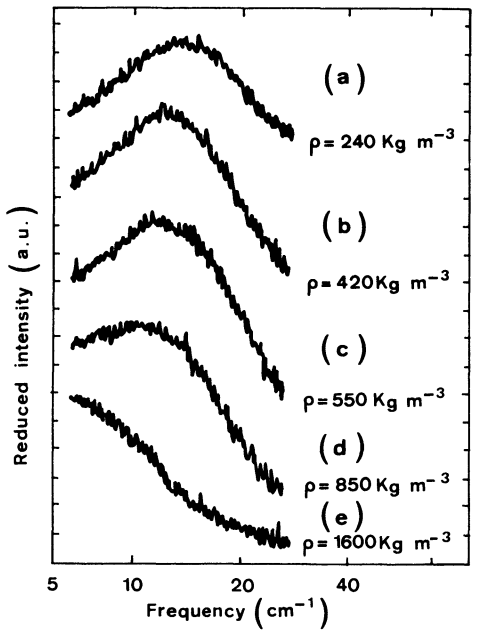

Fig. 3. — Evolution of the low frequency Raman spectra for different times of heat treatment in base catalyzed aerogels. The labels indicate the corresponding densities.

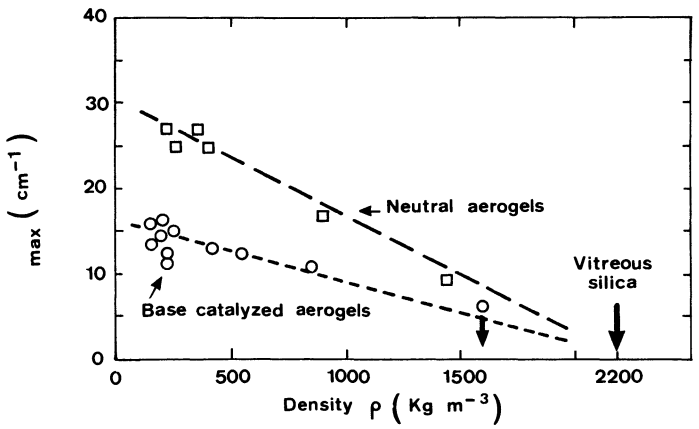

Fig. 4. — Maximum frequency of the peak ν_{max} observed in the low frequency Raman spectra *versus* density for (□) neutral untreated and densified aerogels, (○) base catalyzed untreated and densified aerogels.

vitreous silica which is the final material obtained by densification. The low frequency Raman scattering spectrum for the fully-densified aerogel, shown in figure 2d, is very similar to that of bulk vitreous silica.

SANS data published previously [23] in the same samples allow a determination of the characteristic size of the particles constitutive of the silica gels, which can be correlated to the frequency of vibrational modes. In the $I(q)$ curves a crossover from q^{-D} to q^{-4} dependence

has been observed in aerogels. It gives an estimation of the gyration radius R_g of a particle, as $qR_g \sim 1$ at the crossover. In figure 5 we have plotted the maximum frequency of the peak observed in Raman susceptibility *vs.* R_g^{-1} deduced from SANS experiments. Within the accuracy of the experiments, the two quantities appear proportional. Independently of any model, this result is, to our knowledge, the first direct and convincing evidence for a correlation between the low frequency Raman spectra and a structural information on aerogels.

Assuming that the relation between R_g and ν_{max} is given by equation (1), the measurements of both R_g and ν_{max} can thus be used to obtain an estimate of the sound velocities *at the particle scale.* The quantity

$$v = 2 \times \frac{\nu_{max}}{0.8} R_g \sqrt{\frac{5}{3}} \tag{2}$$

is plotted *vs.* $R = R_g \sqrt{\frac{5}{3}}$ in figure 6. The somewhat large scattering of points originates from uncertainties in the determination of R_g. However, we can deduce a mean velocity $v \simeq 2\,150$ m.s^{-1}. This value is significantly lower than the transverse velocity of sound in vitreous silica ($\sim 3\,700$ m.s^{-1}) and implies an excess Debye density of states than in bulk silica ; as a matter of fact an excess has been really observed by neutron scattering investigation [24] which can be related to this low value of the sound velocity. The low value for the sound velocity at the particle scale can be related to an internal structure different from that of vitreous silica, indicating a more open structure or a residual *microporosity* in the aerogel particle. The nearly constant value found for the velocity (Fig. 6) would imply that this microporosity is identical whatever the catalysis conditions, and remains in the first densification stages. Some indications for differences between the local structure of bulk vitreous silica and that of aerogels have been observed in the high-frequency part of the

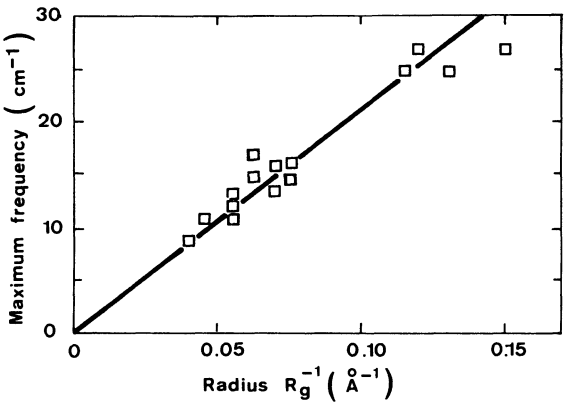

Fig. 5.

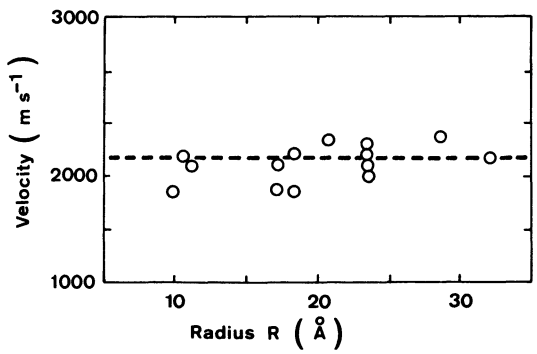

Fig. 6.

Fig. 5. — Maximum frequency of the peak ν_{max} observed in the low frequency Raman spectra *versus* the inverse gyration radius of the particules constituve of the aerogels. R_g^{-1} was deduced from the small angle neutrons scattering results [23]. The results concerns neutral, base catalyzed untreated and also densified samples.

Fig. 6. — Sound velocities v in the elementary particles of the aerogels *versus* their mean size. v is calculated using equation (2) as explained in the text.

Raman spectrum [25]. Moreover, an analysis in terms of composite structure of the elastic moduli of silica gels leads to a similar conclusion [26].

Another explanation for this discrepancy could be that the numerical factor in equation (2) is inadequate. This factor depends on the shape of the particle. The value 0.8 is relevant to spherical particles, while for particles of different shape the numerical coefficient is not known. The relation (2) can be also erroneous if the particles are coupled. However, it is worth noticing that the data points in figure 5 for neutrally reacted and base catalyzed aerogels collapse on the same straight line. As electron microscopy has demonstrated very different particle shapes for these two kinds of samples [27], the above explanation appears unlikely. Nevertheless, the *total* frequency spectrum of the small particles, including surface and bulk modes as calculated for instance by Tamura [28], should be taken into account. In that case the relations (1) and (2) appear a crude approximation. A detailed quantitative analysis of the peak position needs more information on the shape of the particle and coupling of the particles.

Finally, we discuss the temperature dependence of the low frequency Raman spectra of silica aerogels. We studied the temperature dependence of the Raman spectrum on one particular sample with $\rho = 240$ kg.m^{-3}, prepared under basic conditions. We first analyzed the Stokes and the anti-Stokes part of each spectrum, comparing the ratio of intensities on both sides at a given frequency to the expected value of $[n(\omega) + 1]/n(\omega)$. We numerically adjusted the value of the temperature to obtain the superposition of the Stokes and anti-Stokes part of the spectrum. The value of the temperature T obtained in this way is systematically higher by a few degrees that given by a thermometer fixed on the sample. When the sample holder is immersed into liquid helium the above determination gives $T = 20$ K, which is the lowest temperature obtained in this experiment. The comparison of the Stokes Raman spectra at 300 K and 20 K is given in figure 7, where the curves have been shifted arbitrarily along the ordinate axis. The insert in this figure shows the corresponding susceptibilities $\chi(\omega)$, in log-log plot. The two features of each spectrum are a base line with a power-law dependence of the intensity *vs.* frequency and a superimposed well-defined peak.

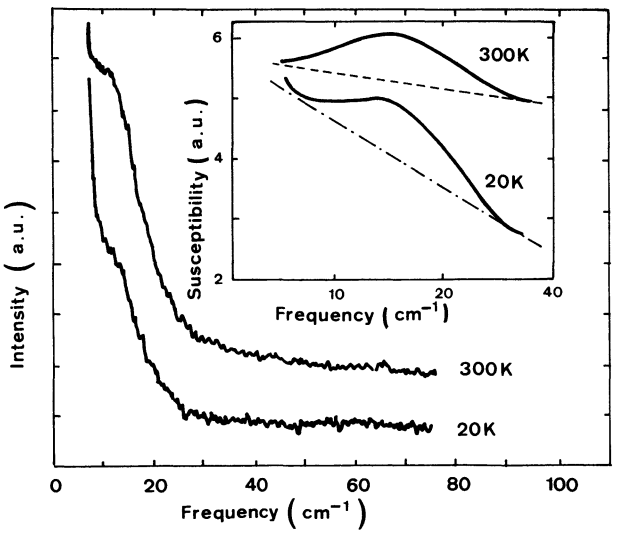

Fig. 7. — Comparison of the law frequency Raman spectra for a base catalyzed sample ($\rho = 240$ kg.m^{-3}) at 300 and 20 K. The insert is a log-log plot of $\chi(\omega)$ in the peak region.

The background power-law dependence in this range of frequency has been attributed previously [29] to fractons at length scales lower than the particle size. Without any confirmation of a fractal geometry or connectivity inside the particle, such an assignment seems questionable and asks for further investigations. Furthermore, the poor signal-to-noise ratio at low temperature, a fluorescence background and a residual elastic scattering which add to the Raman intensity in our experiment makes it difficult to conclude about the temperature dependence of this power-law background. On the other hand we note that neither the shape, nor the frequency position of the peak vary with temperature. This similarity demonstrates the harmonic character of the vibrational modes related to these peaks. The result confirms the previous observation deduced from the temperature dependence of the inelastic neutron scattering signal for lower frequencies [24] or for the nearly same frequency range [30].

References

[1] See, e.g. Phonon Scattering in Condensed Matter, Eds. A. C. Anderson and J. P. Wolfe (Springer, Berlin) 1986.

[2] See, e.g. Amorphous Solids, Low-Temperature Properties, Eds. W. A. Phillips, *Topics in Current Physics* Vol. 24 (Springer, Berlin) 1981.

[3] ANDERSON P. W., HALPERIN B. I. and VARMA C. M., *Philos. Mag* **25** (1972) 1 ; PHILLIPS W. A., *J. Low Temp. Phys.* **7** (1972) 351.

[4] HUNKLINGER S. and SCHICKFUS M. V., in reference [2].

[5] SIEVERS A. J. and TAKENO S., *Phys. Rev. B* **39** (1989) 3374.

[6] BUCHENAU U., NÜCKER N. and DIANOUX A. J., *Phys. Rev. Lett.* **53** (1984) 2316.

[7] BUCHENAU U., PRAGER M., NÜCKER N., DIANOUX A. J., AHMAD N. and PHILLIPS W. A., *Phys. Rev. B* **34** (1986) 5665.

[8] BUCHENAU U., ZHOU H. M., NÜCKER N., GILROY K. S. and PHILLIPS W. A., *Phys. Rev. Lett.* **60** (1988) 1318.

[9] ALEXANDER S. and ORBACH R., *J. Phys. France Lett.* **43** (1982) L625.

[10] ALEXANDER S., LAERMANS C., ORBACH R. and ROSENBERG H. M., *Phys. Rev. B* **28** (1983) 4615.

[11] See, e.g., GRAEBNER J. E., GOLDING B. and ALLEN L. C., *Phys. Rev. B* **34** (1986) 5696 ; GRAEBNER J. E. and GOLDING, *ibid.*, 5788.

[12] ROSENBERG H. M., *Phys. Rev. Lett.* **54** (1985) 704 ; PAGE J. H. and MCCULLOCH R. D., *Phys. Rev. Lett.* **57** (1986) 1324 ; DIANOUX A. J., PAGE A. J. and ROSENBERG H. M., *Phys. Rev. Lett.* **58** (1987) 886 ; FRELTOFT T., KJEMS J. and RICHTER D., *Phys. Rev. Lett.* **59** (1987) 1212.

[13] BOUKENTER A., CHAMPAGNON B., DUVAL E., DUMAS J., QUINSON J. F. and SERUGHETTI J., *Phys. Rev. Lett.* **57** (1986) 2391.

[14] DUVAL E., MARIOTTO G., MONTAGNA M., PILLA O., VILIANI G. and BARLAND M., *Europhys. Lett.* **3** (1957) 333.

[15] FONTANA A., ROCCA F. and FONTANA M. P., *Phys. Rev. Lett.* **58** (1987) 503.

[16] ALEXANDER S., ENTIN-WOHLMAN O. and ORBACH R., *Phys. Rev. B* **32** (1985) 6447.

[17] SCHAEFER D. W. and KEEFER K. D., *Phys. Rev. Lett.* **56** (1986) 2199.

[18] VACHER R., WOIGNIER T., PELOUS J. and COURTENS E., *Phys. Rev. B* **37** (1988) 6500.

[19] DOS SANTOS D. I., AEGERTER M. A., CRAIEVICH A. F., LOURS T. and ZARZYCKI J., *J. Non-Cryst. Solids* **95-96** (1987) 1143.

[20] COURTENS E., PELOUS J., PHALIPPOU J., VACHER R. and WOIGNIER T., *Europhys. Lett.* **6** (1988) 245.

[21] TSUJIMI Y., COURTENS E., PELOUS J. and VACHER R., *Phys. Rev. Lett.* **60** (1988) 2757.

[22] ILLER R. K., The Chemistry of Silica (Wiley, New York) 1979.

[23] VACHER R., WOIGNIER T., PHALIPPOU J., PELOUS J. and COURTENS E., *Revue Phys. Appl.* **24** (1989) C4.

[24] REICHENAUER G., FRICKE J. and BUCHENAU U., *Europhys. Lett.* **8** (1989) 415.

[25] WALRAFEN G. E., HOKMABADI M. S., HOLMES N. C., NELLIS W. T. and HENNING S., *J. Chem. Phys.* **82** (1985) 2472.

[26] MURTAGH M., GRAHAM E. and PANTANO C., *J. Am. Ceram. Soc.* **69** (1986) 775.

[27] BOURRET A., *Europhys. Lett.* **6** (1988) 731.

[28] TAMURA A., HIGETA K. and ICHINOKAWA T., *J. Phys. C. Solid State Phys.* **15** (1982) 4975 ; TAMURA A. and ICHINOKAWA T., *J. Phys. C. Solid State Phys.* **16** (1983) 4779.

[29] ROUSSET J. L., DUVAL E., BOUKENTER A., CHAMPAGNON B., MONTEIL A., SERUGHETTI J. and DUMAS J., *J. Non-Cryst. Solids* **107** (1988) 27 ; BOUKENTER A., CHAMPAGNON B., DUVAL E., ROUSSET J. L., DUMAS J. and SERUGHETTI J., *J. Phys. C. Solid State Phys.* **21** (1988) L1097.

[30] VACHER R., WOIGNIER T., PELOUS J., CODDENS G. and COURTENS E., *Europhys. Lett.* **8** (1989) 61.